International journal of scientific and technical research in engineering (IJSTRE)
www.ijstre.com Volume 2 Issue 6 ǁ June 2017.

Effective removal of dye Alizarin Red S using CTAB modified PVA-Alginate bound nano magnetite microspheres

Alka Tiwari* & Prerna Kathane

Research Centre: Department of Chemistry
Government Vishwanath Yadav Tamskar Post Graduate
Autonomous College, Durg (Chhattisgarh) 491001, INDIA

ABSTRACT: *Present study aims to investigate the efficiency of newly synthesized adsorbent polyvinyl alcohol-alginate bound nano magnetite microspheres modified with cetyltrimethyl ammonium bromide [PVA-ANM/CTAB] in removal of anionic dye 'Alizarin Red S' from aqueous medium. The effect of agitation time, influence of pH, amount of adsorbent, initial dye concentration and temperature were systematically studied by batch sorption system. Various isotherms and kinetic models have been fitted with experimental data to evaluate mechanism of adsorption. Characterization of the so-prepared adsorbent was accomplished by FTIR, XRD, SEM and TEM analysis. The experimental data fitted very well with Freundlich and Temkin isotherm model. The sorption kinetics follows pseudo second order kinetic model. PVA-ANM/CTAB has been found an effective, economic, eco-friendly and efficient adsorbent as it showed ≥ 98% removal at pH 8 and could be regenerated by acetic acid and reused.*

KEYWORDS: *Alizarin Red S, Nano magnetite, polyvinyl alcohol-alginate, sorption efficiency, sorption isotherm,*

I. INTRODUCTION

Urbanization activities and rapid industrialization has been exploited natural resources of water worldwide. Various kinds of synthetic dyes are commercially available, among them reactive anthraquinone dyes are extensively employed in the textile industries due to their wide range of color shades and ease of application. Dyes have also been used in paper, plastic, leather, cosmetic, pharmaceutical and food industries, which generate huge volume of industrial wastewater having dye contamination per annum. Dyes are the derivative of aromatic compounds, having halo, nitro and sulfo groups in their structure are toxic, mutagenic and carcinogenic in nature. Complex molecular structure and fused aromatic ring structure are the main cause of their inherent chemical stability and non biodegradable nature [1]. Recently much attention has been paid for the elimination of dye contamination from industrial wastewater because most of dyestuffs are harmful to human beings and aquatic environment even at very low concentration. Persons having skin allergies are more susceptible to its hazardous effects. Its acute toxicity leads to irritation to skin, eyes, lungs, mucous, membranes and gastro intestinal tract, asthma and in chronic condition it leads to dermatitis. Therefore the removal of toxic dye from wastewater before discharge into the environment seems to be essential for economical and environmental point of view [2]. Several treatment methods like biodegradation, ion exchange, reverse osmosis, adsorption, membrane filtration, nano filtration and electrochemical separation have been applied to remove dyestuffs from industrial effluents. Among these methods adsorption has been recognized to one of the promising techniques due to its effectiveness, simplicity, easy to operation and wide ranging availability [3, 4]. In earlier various biological materials, biomaterial based synthetic and magnetically modified adsorbent like rice-husk [5], fly ash and red mud [6], activated carbon, rambutan peel based activated carbon [7-9], alginate/PVA kaoline composite [10], magnetically modified spend coffee grounds [11], magnetic fluid modified peanut husks [12], Chitosan and Chitosan nanoparticles [13,14], nano iron-oxide loaded alginate[15] etc has been reported to eliminate the azo dyes from aqueous solutions. However these adsorbents do not have good adsorption capacities towards acid dyes due to the presence of negatively charged functional groups on their surfaces. Therefore in order to improve the adsorption capacity of these sorbents, surface modification using cationic surfactants treatment seems to be an effective method. It was reported that the cationic surfactants mostly quaternary ammonium salts like hexadecyl trimethyl ammonium [HDTMA] or cetyltrimethyl ammonium bromide [CTAB] provided potential positively charged active sites for efficient removal of anionic contaminants from aqueous solutions [16,17].

In present paper, removal of anionic dye 'Alizerin Red S'[ARS] from aqueous solution was investigated using polyvinyl alcohol-alginate bound nano magnetite microspheres modified with cetyltrimethyl ammonium bromide [PVA-ANM/CTAB] by batch method. Polyvinyl alcohol [PVA] is low-cost, durable, nontoxic, biodegradable and biocompatible synthetic hydrophilic polymer. Alginate is a polysaccharide having high affinity and binding capacity for several toxicants uptake from aqueous solutions have been reported for possible applications in water treatment process. The use of nano magnetite particles of iron oxide with CTAB modified PVA-alginate provides large surface area with very strong sorption ability. The strong magnetic and cationic properties of sorbent opens a new technology, which is quicker, simpler and more precise than those used traditionally. It has been reported that morphology of microspheres beneficial to mass diffusion and transport in solution [18]. Combined technique of magnetic separation and adsorption process has benefits of flexibility and ecofriendly characteristics as compared to other reported technology used for elimination of anionic dyes. Mechanism of sorption technique are discussed. Regeneration and reused study related with desorption/adsorption cycles also performed. ARS (1, 2 dihydroxy-9, 10 anthraquinone sulfonic acid salt) is water soluble, odorless, orange-red colored, widely used anthraquinone dye having molecular weight 342.257and molecular formula $C_{14}H_7O_7SNa$, structure illustrated in Fig.1.

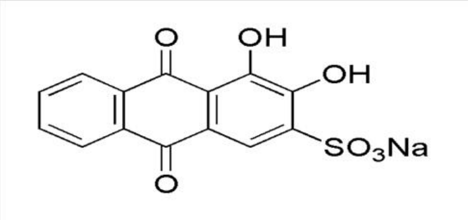

Fig. 1 Structure of Alizerin Red S dye

II. EXPERIMENTAL

2.1. Materials: Ferric chloride anhydrous, ferrous chloride tetrahydrated, Alizerin Red S ($C_{14}H_7O_7S_7Na$) were purchased from Central Drug House, New Delhi, India. CTAB, sodium alginate, polyvinyl alcohol were purchased from Loba Chemie, Mumbai, India of analytical grades and used without any purification. Doubled distilled water was used throughout the experiments.

2.2. Preparation of nano magnetite microspheres of PVA-A/ CTAB**:** The adsorbent were prepared in three steps, in first step a viscous gel of polyvinyl alcohol (PVA) was prepared at 90^{o}C in doubled distilled water and was mixed thoroughly with the gel of sodium alginate and CTAB to get 1:1:1/9 ratio, stirred for three hours for homogeneity and kept aside to obtain a bubble free solution. In second step the microspheres were prepared by drop wise addition of the above mixture in $CaCl_2$ solution (0.5M) for cross linking. The microspheres so produced were allowed to harden by leaving them in solution for 24 hours then washed several times with distilled water. In the third step for insitu magnetization, these microspheres were kept in an aqueous solution of ferrous chloride tetrahydrate and ferric chloride in 1:3ratio for 24 hours. The microspheres were then added into ammonia solution and kept for 2 hours, so that the Fe^{2+}/Fe^{3+} ions get precipitated into nano magnetite iron-oxide within the CTAB-PVAA matrix. These PVA-ANM/CTAB microspheres were then completely washed several times and stored for adsorption studies. PVA-ANM/CTAB microspheres were shown in Fig. 2.

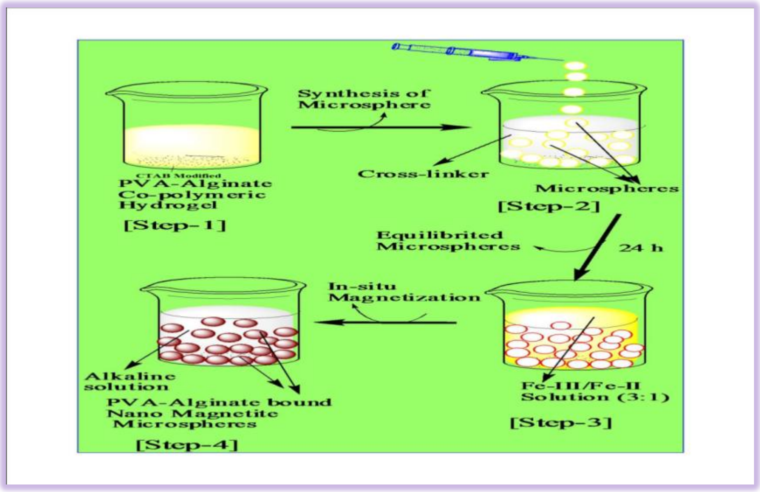

Fig.: 2 Preparation steps of PVA-ANM/CTAB microspheres

2.3. Batch Adsorption Experiments: A Stock solution of dye 'Alizerin Red S' (ARS) 1000 mg/L was prepared and the operating solutions were prepared by diluting the stock solutions. The adsorption experiments were carried out by batch method by varying shaking time, pH scale, concentration of adsorbate, mass of adsorbent and temperature. For adsorption experiments, the PVA-ANM/CTAB microspheres 0.25g and 25ml 'ARS' solution of 25mg/L concentration at pH 8 and temperature 25°C was stirred in an orbital shaking incubator with temperature control (SONAR-159) at 200 rpm for 150 min. The amount of 'ARS' dye present in solution (before and after equilibrium adsorption) was determined by using UV-visible spectrometer (Systronics-117). The sorption degree (removal efficiency) and sorption capacity of the sorbent were calculated according to Eq. 1 and 2, respectively:-

$$Sorption\ degree = \frac{C_i - C_e}{C_i} \times 100\% \qquad (1)$$

$$\text{Sorption Capacity} = \frac{\mathrm{C_i - C_e \times V}}{\mathrm{m}} \qquad (2)$$

where C_i and C_e (mg/L) are initial and equilibrium concentration of 'ARS' dye solution, respectively. V (L) is volume of adsorbate solution, subjected to sorption and m (g) is weight of adsorbent.

Desorption Study: After adsorption experiments, ARS loaded PVA-ANM/CTAB microspheres was collected by filtration, washed and desorption study conducted with acetic acid of distinct strength ranging from 0.05 to 0.3 M. Desorption efficiency was evaluated by Eq.3.

$$Desorption\ efficiency = \frac{Amount\ \ of\ dye\ ARS\ desorbed}{Amount\ \ of\ dyeARS\ adsorbed} \times 100 \qquad (3)$$

2.4. Characterization of adsorbent

2.4.1**. XRD** Analysis: The crystalline nature of PVA-ANM/CTEB adsorbent was studied on a Brucker D8 advanced X-ray diffractometer with scanning range from 20^o to 80^o (2θ) using Cu-Ka radiation with wavelength of 1.5406 A^o.

2.4.2 **SEM** Analysis: The morphological and size of the PVA-ANM/CTAB adsorbent before and after 'ARS' dye adsorption, samples were viewed using a scanning electron microscope.

2.4.3. **FTIR** Analysis: Characteristics functional groups present on adsorbent PVA-ANM/CTAB before and after adsorption were recorded by Perkin–Elmer FTIR spectrophotometer.

2.4.4**. TEM** Analysis: The average particle size, morphology and size distribution of iron-oxide nanoparticles were examined using TECNAI-G-20 TEM at a voltage of 200 KV.

III. RESULTS & DISCUSSIONS

3.1. Characterization of PVA-ANM/CTAB adsorbent

3.1.1. **XRD Analysis**

Powder XRD was carried out to identify the nanocrystalline structure of the iron-oxide and the amorphous nature of PVA-ANM/CTAB. Fig. 3 showed five characteristics peaks (2θ=26.93, 31.89, 38.87, 41.23 and 45.55). The position and relative intensities of all diffraction peaks match well with those from the JCPDS file number 89-5984 for nano magnetite Fe_3O_4 and reveal that the prominent phase formed is Fe_30_4 with resultant nanoparticles of pure magnetite with boxy structure. Nano magnetite particles are obtained according to the reaction:-

$$2FeCl_3 + FeCl_2 + 8NH_4OH \rightarrow Fe_3O_4 + 8NH_4Cl + 4H_20$$

3.1.2. **FTIR Analysis**

Numerous chemical groups have been proposed to be responsible for the adsorption of dye such as carboxyl, hydroxyl and amino group. FTIR spectra of adsorbent before (a) and after adsorption of dye ARS (b) displayed in Fig. 4. Their relative importance in dye sorption may depend on factor such as the quantity of sites, accessibility, chemical state and affinity between site and dye. The vibrancy signals of adsorbent before and after sorption of 'ARS' dye were different, indicates bands close to 3460 cm^{-1} due to –OH stretching in carboxyl group and near 1609 cm^{-1} due to C=O asymmetrical stretching of –COOH group and near 1540cm^{-1} due to $-NH_2$ group. The band at 1086 cm^{-1} is attributed to the –C-O stretching. There is an obvious absorption band at the low frequency zone of 450-750 cm^{-1}, which is assigned to the stretching vibration of the Fe-O band in iron oxide. The characteristic peak at 529.21 cm^{-1} relates to Fe-O group, which indicates the loading of nano iron oxide particles on adsorbent by the electrostatic interaction and chemical reaction through cross-linker. By comparing the spectra of magnetite microspheres before adsorption and after adsorption, the following conclusions could be drawn. The shifting of –OH stretching band from 3385 to 3460 cm^{-1} suggests the attachment of adsorbate dye. The shifting of the C-O band to the lower frequency from 1034 to 1027 cm^{-1} can be attributed to the association of the hydroxyl group with adsorbate dye and shifting of $–NH_2$ band from 1540 to 1515 cm^{-1} suggests the attachment of adsorbate. A slight shift of Fe-O band from 495 to 517 cm^{-1} shows the adsorption of some of the adsorbate dye ARS onto the nano iron-oxide surface.

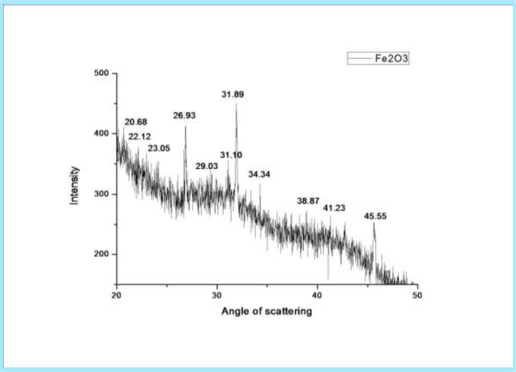

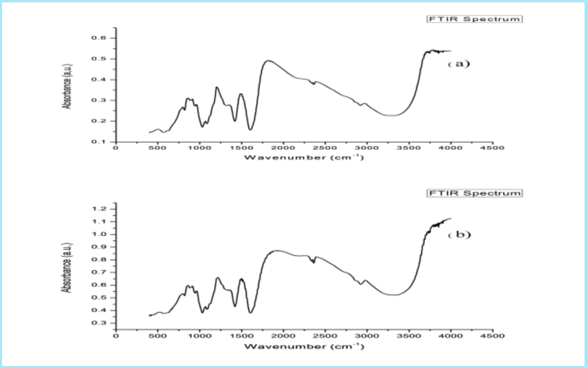

Fig. 3 XRD Image of PVA-ANM/CTAB

Fig. 4 FTIR spectra of adsorbent

3.1.3. SEM Analysis

SEM images of adsorbent PVA-ANM/CTAB were obtained for before and after adsorption of dye are revealed in Fig. 5(a) and (b), respectively. It is clearly visible from image that the constituted co-polymeric nano magnetite particles of adsorbent are not compatible and hence resulted in a blend of heterogeneous surface and has porous morphological view. The surface of adsorbent has covered by adsorbate and become smooth after adsorption.

3.1.4. TEM Analysis

TEM images of nanoparticles Fig. 6 shows almost spherical iron-oxide particles with an average size between 2 to7 nm. It should be noted however, that the majority of particles were scattered, a few of them showing aggregates indicates stabilization of the nanoparticles

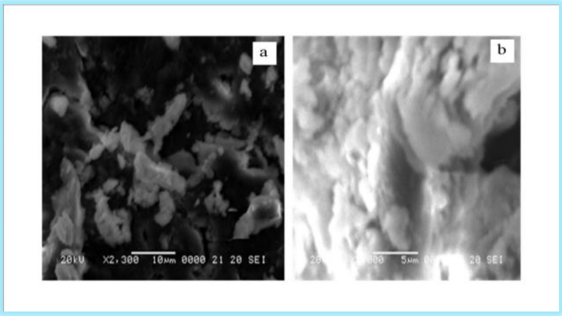

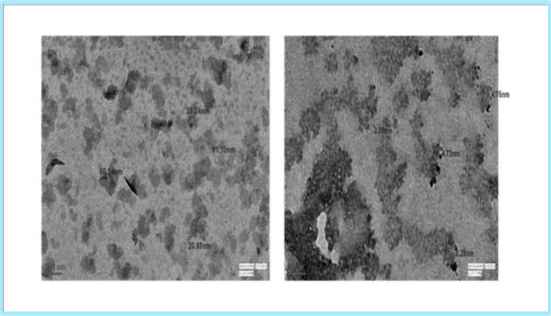

Fig. 5 SEM images of PVA-ANM/CTAB

Fig. 6 TEM images of PVA-ANM/CTAB

3.2. Adsorption Isotherms

The parameters obtained from the different models provide important info on the adsorption mechanism and also the surface properties of the adsorbent and the design of adsorption systems. Adsorption isotherms, ascribes how adsorbate molecules interact with adsorbent particles and are thus critical in optimizing the use of chemically modified solid materials. The experimental data were compared by applying most widely accepted adsorption equilibrium models Langmuir and Freundlich isotherm models.

3.2.1. Langmuir Isotherm: The empirical non linear Langmuir isotherm model is given by Eq.4:-

$$\frac{q_e}{q_m} = \frac{K_L C_e}{1+K_L C_e} \qquad (4)$$

where q_e is dye concentration on adsorbent at equilibrium(mg/g), C_e is the dye concentration in solution at equilibrium(mg/L), q_m is adsorption capacity of adsorbent(mg/g) and K_L the Langmuir adsorption constant related to energy (L/mg) . The linearized equation of Langmuir is represented as follows:-

$$\frac{1}{q} = \frac{1}{qm} + \frac{1}{K_L\, q_m\, C_i} \qquad (5)$$

where C_i is the initial dye concentration (mg/L). The value of K_L and q_m were calculated by the slope and intercept of the plot between 1/q and 1/C_i, respectively. The essential characteristics of Langmuir isotherm can be expressed in terms of dimensionless constant called separation factor R_L, is defined by Eq.6:-

$$R_L = \frac{1}{K_L q_m C_i} \qquad (6)$$

The value of this parameter indicated the shape of the isotherm, for in which $R_L>1$ is unfavorable, $R_L=1$ is linear, $0< R_L< 1$ is favorable and $R_L=0$ is irreversible. In present sorption systems R_L value was obtained 0.323 proves favorable adsorption of dye on PVA-ANM/CTAB.

3.2.2. Freundlich Isotherm: The Freundlich isotherm model can be applied for non ideal adsorption on heterogeneous surfaces and multilayer adsorption. Its basic assumption is that non-uniform distribution of adsorbate on heterogeneous surface with physio-sorption. Linear form of the Freundlich isotherm model is given by Eq. 7

$$log q_e = log K_F + \frac{1}{n} log C_e \qquad (7)$$

where q_e is amount of dye adsorbed per unit of adsorbent (mg/g), C_e is the dye concentration in solution at equilibrium (mg/L), K_F and 1/n are Freundlich empirical parameter related to multilayer adsorption capacity and adsorption intensity, respectively. K_F and 1/n may be obtained from the linear plot of log q_e versus log C_e, as depicted in Fig. 7 (b). Value of n is 0.502 (>1) it also indicated the favorable adsorption of dye on adsorbent PVA-ANM/CTEB.

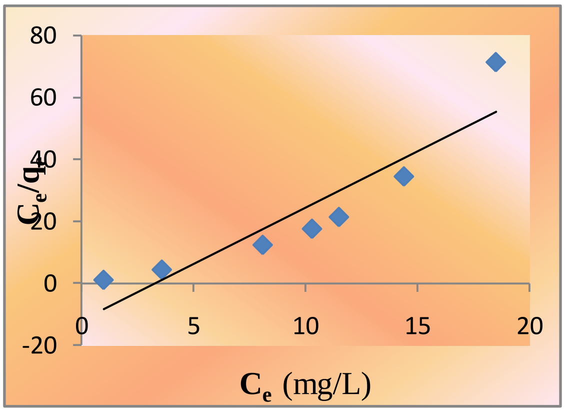

Fig 7(a) Langmuir Isotherm

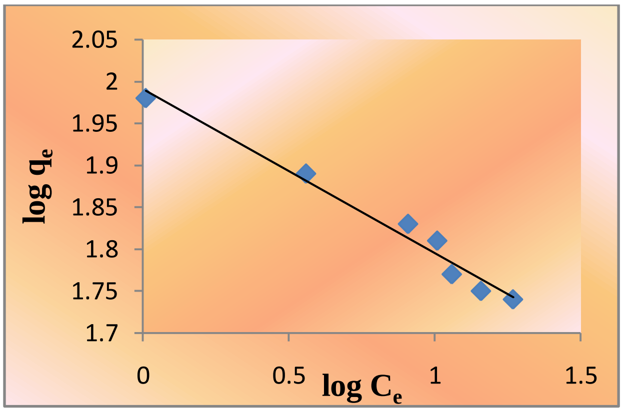

Fig 7(b) Freundlich Isotherm

Table 1 Values of Langmuir and Freundlich isotherm of dye ARS Uptake on PVA-ANM/CTAB

Langmuir Isotherm				**Freundlich Isotherm**		
q_m	K_L	R^2	R_L	K_F	n	R^2
118.6	0.084	0.839	0.323	5.128	0.502	0.975

3.3. Adsorption Kinetic Study

Adsorption kinetic study provides valuable insights information of reactions pathway. The three most commonly used kinetic models suggested by Lagergren, Ho McKay and Weber & Morris.

3.3.1. Pseudo-first order kinetic model: Lagergren proposed pseudo-first order kinetic model. Integral form of model is given by Eq. 8:-

$$log(q_e - q_t) = log q_e - \frac{K_{ad}}{2.303} t \qquad (8)$$

where q_e and q_t are the adsorption capacity (mg/g) at any time (t) and equilibrium, respectively. K_{ad} is the pseudo-first orders rate constant of adsorption, calculated from linear plot of log (q_e-q_t) versus t, values are listed in Table 2.

3.3.2. Pseudo-second order kinetic model: The linear integral form of the pseudo-second order kinetic model (Ho McKay model) is:-

$$\frac{t}{q_t} = \frac{1}{k_2' q_e^2} + \frac{1}{{q_e}^2} t \qquad (9)$$

where $k_2'q_e^2$= h (mg/g. min) can be regarded as initial adsorption rate when t→0 and k_2' is the rate constant of pseudo-second order kinetics. The plot of t/q_t versus t gave a straight line, $q_e^2$and h can be determined from slope and intercept, respectively as depicted in Fig. 6 (b). Values are given in Table 2. The best fit to the pseudo-second order kinetics indicates that the adsorption mechanism depends on adsorbate and adsorbent [19, 20].

3.3.3. Intraparticle Diffusion: Kinetics sorption of a material on to sorbent follows three steps i.e., pore diffusion, film diffusion and intraparticle transport. Mostly pore diffusion is rate limiting step during batch process [21, 22]. Thus in order to evaluate rate controlling step plot was drawn between adsorbed amounts of dye on adsorbent q_t vs. $t^{1/2}$ as depicted in Fig. 6(c), intraparticle diffusion rate constant K_p (gm/g. min$^{1/2}$) was determined from linear portion of curve by Morris Weber Eq. 10:-

$$q_t = K_p t^{1/2} + C \qquad (10)$$

Adsorption follows intraparticle diffusion with R^2 0.935 proved physical phenomenon impact.

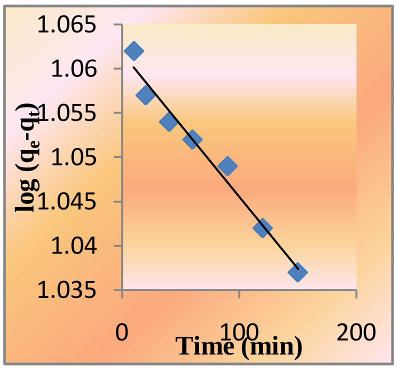

Fig. 6(a) Pseudo-I order model

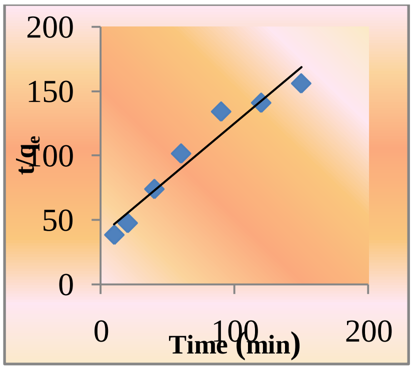

Fig. 6(b) Pseudo-II order model

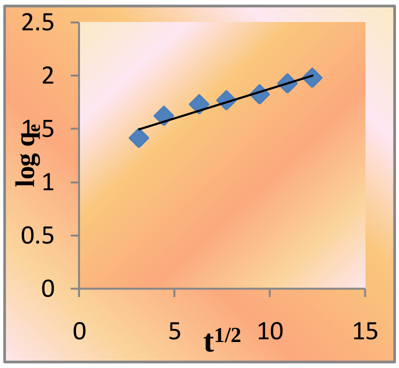

Fig. 6(c) Intraparticle Diffusion

Table 5.2 Results of Kinetic parameters for Dye ARS Uptake on PVA-ANM/CTAB

Pseudo First Order Model			Pseudo Second Order Model				Intraparticle Diffusion	
qe mg/g	k_1 min^{-1}	R^2	qe^2 mg/g	k_2 /mg min	h mg/g min	R^2	Kp g /mg min$^{-0.5}$	R^2
8.00	0.005	0.640	1.311	0.029	14.973	0.944	0.055	0.935

3.4. Sorption Mechanics of 'ARS' dye onto PVA-ANM/CTAB

Surface characteristics of PVA-ANM/CTAB adsorbent and pH of solution plays an important role adsorption. At pH 8 if the acid-base interaction were the key sorption mechanism, anionic pollutants may be expected to have larger affinity to group of adsorbent [23-25]. The most suitable mechanism of dye ARS adsorption onto PVA-ANM/CTAB may be expressed in Fig. 7. The cross-linked polyvinyl alcohol-alginate contains oxalate (--O-), carboxylate (---COO-) and hydroxyl (--OH-) groups. When these co-polymeric matrix of PVA-Alginate modified with cetyl trimethyl ammonium bromide (CTAB), the hydrophobic groups of CTAB interact and attached with carboxyl ate (a), hydroxyl (b) and oxalate (c) groups respectively. Dye 'ARS' attached with cationic ammonium ( ) group of CTAB by electrostatic interaction. In addition with electron deficient nano magnetic iron-oxide particles with in PVA-A/CTAB co-polymeric matrix may be co-ordinate by sulphonate group of 'ARS' dye (d).

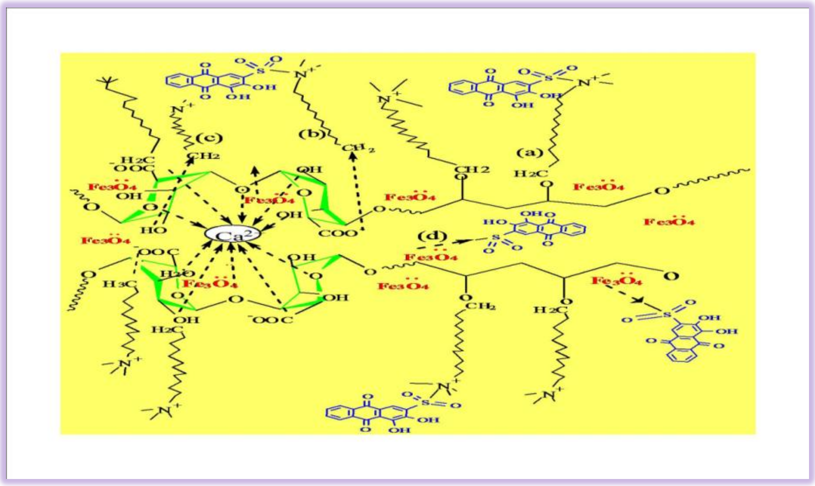

Fig. 7. Mechanism of 'ARS' dye Adsorption onto PVA-ANM/CTAB

3.5. Factor affecting adsorption of dye 'ARS' onto PVA-ANM/CTAB microspheres

Effect of pH: The effect of pH on uptake of dye was analyzed within the range between 2 to 12 as shown in Fig. 8(a). The maximum adsorption ≥ 98% observed at pH 8, because surface charge of adsorbent become negative due to the deprotonation of the phenolic group present in 'ARS' dye solution and the removal efficiency of adsorbent will get a significant enlargement.

Effect of Adsorbent dose: The impact of adsorbent dose on adsorption of dye were studied by varying amount of adsorbent from 0.05 to 0.30 g using a fixed dye concentration of 25mg/L for 150 min, as shown in Fig. 8(b). Maximum sorption occurred at adsorbent dose of 0.25g. Increasing of adsorption with increasing of adsorbent dose will be owing to the more availability of free binding sites.

Effect of Time: Agitation time is one of the important factors in adsorption process. The removal of 'ARS' dye was studied as a function of contact time in the range between 10 and 240 minutes. The results depicted that with the increase of contact time the percentage adsorption also increased. The maximum removal obtained at 150 min, as shown in Fig.8(c).

Effect of Concentration: Effect of initial ARS dye concentration on adsorption was studied in the range of 5 to 50 mg/L. Adsorption percentage increased with increase in initial dye concentration and found maximum ≥ 96% removal at 25 mg/L as shown in Fig. 8 (d). On increasing the concentration of adsorbate, more ions of the dye arrive at the interface and get adsorbed. At higher concentrations, more dye molecules were left in solution due to saturation of limited binding sites on the adsorbent [26].

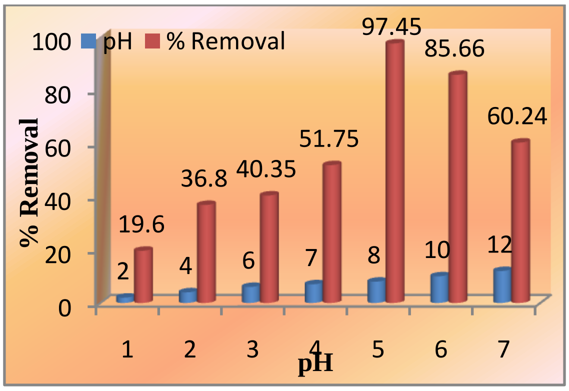

Fig. 8(a) Effect of pH

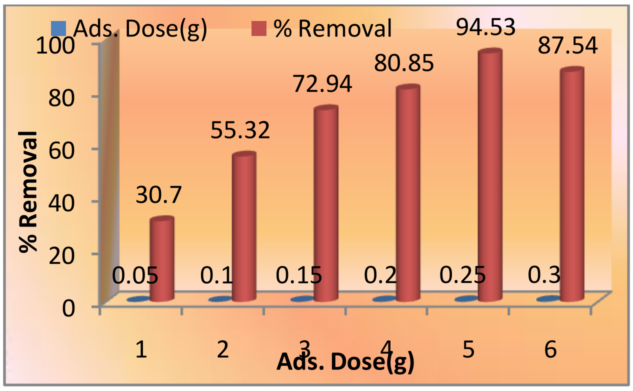

Fig. 8(b) Effect of Adsorbent dose

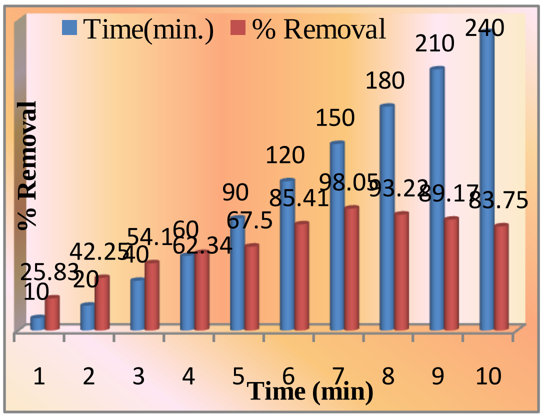

Fig. 8(c) Effect of Time

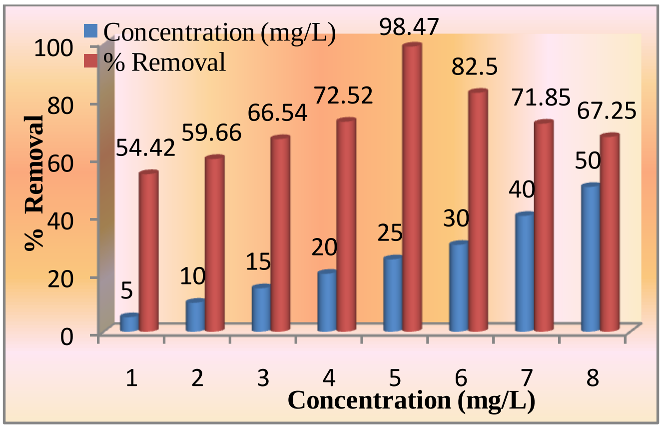

Fig. 8 (d) Effect of Concentration

Effect of Temperature: Effect of temperature on uptake of dye ARS was investigated at various temperature ranged between 15 and 55℃, it is very important for kinetics and thermodynamic point of view. The result is illustrated in Fig. 8 (e). It was observed that maximum removal of dye occurred at 25 ± 2℃ and adsorption yield decreases with increase in temperature because molecules move with great speed and less time of interaction was available for dye anions with adsorbent material, due to decrease in the viscosity of solution [27].

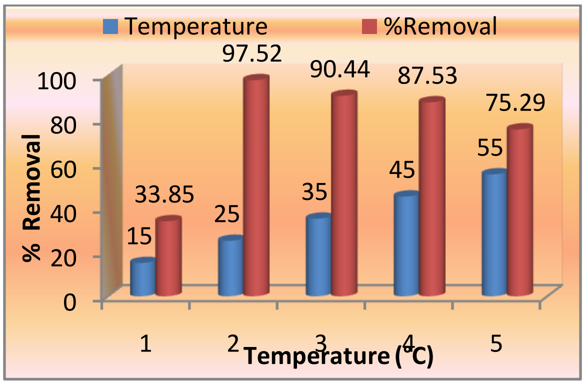

Fig. 8(c) Effect of Temperature

3.6. Desorption and Regeneration Study

An adsorbent will be significant in waste-water treatment when it has good adsorption capacity as well as the regeneration and reused ability in adsorption/desorption cycles. Desorption studies carried out by different concentration of acetic acid ranging from 0.025 to 0.30 M. Maximum desorption ≥99 %, obtained with 0.15M CH_3COOH as shown in Fig. 9(a). For practical applicability of regenerating adsorbent, dye loaded PVA-ANM/CTAB microspheres treated with 0.15M acetic acid by repeating adsorption-desorption process for six regenerating cycles, there was negligible changes observed in initial sorption capability of adsorbent as shown in Fig. 9 (b). Hence PVA-ANM/CTAB sorbent has potential to uptake dye 'ARS' repeatedly from contaminated water.

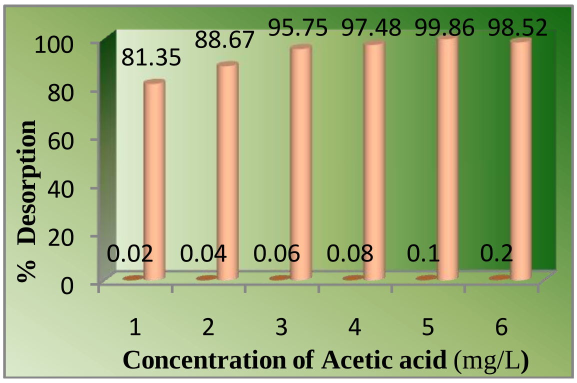

Fig. 9(a) Desorption of Adsorbent

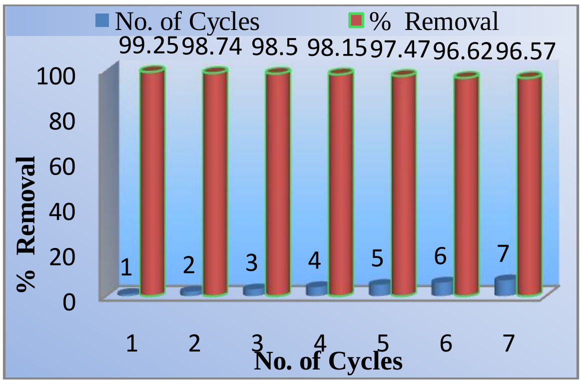

Fig. 9 (b) Regeneration of Adsorbent

IV. CONCLUSIONS

A novel adsorbent PVA-ANM/CTAB microsphere was synthesized by in-situ magnetization and assessed for effective adsorption of ARS dye by batch sorption system. The maximum removal of dye was noticed at pH 8 and 25(±2)^{0}C in 150 min. Sorption data closely fitted with Freundlich isotherm model. The process of adsorption follows the pseudo second order kinetic equation. Results revealed that the physio-sorption is predominant mechanism in surface assimilation. Hence the adsorbent PVA-ANM/CTAB microspheres has been found to be very effective, efficient, ecofriendly and economical adsorbent for the removal of anionic dyes from water and wastewater and could be regenerate and reused several times tracing negligible losses in their initial sorption capability. Results obtained prove that adsorbent has potential as an inexpensive adsorbent for removal and recovery of anionic dyes from contaminated water.

V. ACKNOWLEGMENT

The authors would like to express thanks to UGC-DEA consortium of Scientific Research Centre, Indore, India for FTIR & XRD, SAIF Punjab University, Chandigarh, India for SEM and AIIMS New Delhi, India for TEM analysis.

REFERENCES:-

[1]. A. Gil, F.C.C. Assis, S. Albeniz, and S. A. Korili, "Removal of dyes from wastewaters by adsorption on pillared clays," *Chem. Eng. J.*, 168, 2011, 1032–1040.

[2]. R. Rehman and T. Mahmud, Sorptive elimination of Alizerin Red S Dye from water using Citrullus lanatus peels in environmentally benign way along with equilibrium data modeling, *Asian J. of Chemistry, 25 (10)*, 2013, 5351-5356.

[3]. P. Zucca, C. Vinci, F. Sollai, A. Rescigno and E. Sanjust, "Degradation of Alizerin Red S under mild experimental condition by immobilized 5,10,15,20, tetrakis (4Sulfonate phenyl) porphine Mn (IV) as a biomimatic peroxidax-like catalyst", *J. of Molecular Catalysis A: Chemicals, 288*, 2008, 97-102.

[4] S. Chatterjee, T. Chatterjee, S.R. Lim and S. H. Woo, "Effect of surfactant impregnated into Chitosan hydrogel beads formed by sodium dodecyl sulfate gelation for the removal of Congo red", *Separation Sci. and Tech., 46, 2011* , 2022-2031.

[5] S. Yusra and H.N. Bhatt, "Adsorptive removal of direct dyes by low cost rice husk: Effect of treatments and modifications", *African J. of Biotech., 10(16)*, 2011, 3128-3142.

[6] S.B. Wang, Y. Boyjoo, A. Choueib, Z.H. Zhu, "Removal of dyes from aqueous solution using fly ash and red mud', Water Res. vol. 39, pp. 129-138, 2005.

[7] E. N. El Qada, S. J. Allen and G. M. Walker, "Adsorption of Methylene Blue onto activated carbon produced from steam activated bituminous coal : A study of equilibrium adsorption isotherm," *Chem. Eng. J. 124*, 103–110, 2006.

[8]. S. Gokturk and S. Kalue, "Removal of selected organic compounds in aqueous solution by activated carbon", *J. of Environ. Sci. & Technol., 1(3)*, 2008, 111-123.

[9]. M.A. Ahmed and R. Alrozi, "Removal of malachite green dye from aqueous solution using Rambutan peel based activated carbon", *Chem. Eng. J., 171*, 2011, 510-516.

[10]. M.M. Abe El-Latif, M.F. Elkady, M.E. Ossman, "Alginate/PVA-Kaoline composite for removal of Methylene blue from aqueous solution", *J. of American Sci., vol. 6 (5)*, 2010, 280-292.

[11]. M. Ivo Safarik, K. Horska and B. Svobodova, "Magnetically modified spends coffee grounds for dyes removal", *Eur. Food Res. Technol., 234*, 2012, 345-350.

[12]. I. Safarik and S.M. Safarikova, "Peanut husks magnetic fluid modified as an adsorbent for organic dye removal", *Science Direct Physics Procedia, 9, 2010* , 274-278.

[13]. A. Negrulescu, V.Patrulea, M. Mincea, C. Moraru and V. Ostafe, "The adsorption of tatrazine, congo red and methyl orange on chitosan beads", *Digest J. of nano materials and biostructures , 9 (1)* , 2014, 45-52.

[14]. Z.G. Hu, J. Zhang, W.L. Chan, Y.S. Szeto, "The sorption of acid dye on to chitosan nanoparticles, Polymer", vol. 47(16), pp. 5838-5842, 2006.

[15]. A. Soni, A. Tiwari and A.K. Bajpai, "Removal of malachite green from aqueous solution using nano iron oxide loaded alginate microspheres: batch and column studies", *Research on Chemical Intermediates, DOI 10.1007/s111*64-012-1011-1, 2013.

[16]. S. R. Taffarel and J. Rubio, "Adsorption of sodium dodecyl benzene sulphonate from aqueous solution using a modified natural zeolite with CTAB", *J. Mineral Engineering, 23, 2010,* 771-779,.

[17]. R. Ansari and B. Seyghali, "Cationic surfactants modified wood sawdust for removal of acidic dyes from aqueous solution", *Eur. Chem. Bulletin, vol. 2 (7)*, 2013, 499-506.

[18]. L. M. Guo, L.X. Zhang, J.M. Zhang, j. Zhou, Q.J. He, S.J. Zeng, X. Z. Cui, J.L. Shi, "Hollow mesoporous carbon spheres an excellent bilirubin adsorbent", *Chem. Commun., 40*, 2009, 6071-6073.

[19]. M. Yazdanbakhsh, H. Tavakkoli and S.M. Hosseini, "Characterization and valuation catalytic efficiency of La$_{0.5}$Ca$_{0.5}$NiO$_3$ nano-powders in removal of reactive blue-5 from aqus. Soln.", *Desalination , 281*, 2011, 388-395.

[20]. A. Cristina and Y. Gushikem, "Removal of methylene blue dye from aqueous solutions by adsorption using yellow passion fruit peel as adsorbent", *Bioresour. Technol.,99*, 2008, 3162–3165.

[21]. D. Karadag, M. Turan and E. Akgul, "Adsorption, equilibrium and kinetic of reactive black 5 & reactive red 239 in aqueous solutions onto surfactant modified zeolite", *J. Chemical Engineering data, 52*, 2007, 1615-1620.

[22]. A. Mittal, V. Thakur, J. Mittal, and H. Vardhan, "Process development for the removal of hazardous anionic azo dye Congo red from waste-water by using hen feather as potential adsorbent," *Desalina. & Water Treat., 52* , 2014, 227–237.

[23]. Z. Hasan and S.H. Jhung, "Removal of hazardous organics from water using metal-organic frameworks: Plausible mechanisms for selective adsorbent", *J. of Hazard. Mater., 83*, 2015, 329-339,.

[24]. J. Fu, Z. chen ,M. Wang, S. Liu, J. Zhang, R. Han, Q. Xu ,' "Adsorption of methylene blue by a high-efficiency adsorbent (polydopamine microspheres): Kinetics, isotherm, thermodynamics and mechanism analysis" *Chem. Eng. J., 259*, 2015, 53-61.

[25]. M. Auta and B.H. Hameed, "Chitosan-clay composite as highly effective and low-cost adsorbent for batch and fixed-bed adsorption of methylene blue", *Chem. Eng. J., 237*, 2014, 352-361.

[26]. X. Y. Huang, B.J. Ping, H. Tian Bu & G.B. Jiang, "Removal of anionic dye eosin Y from aqus. Soln. using ethylenediamine modified chitosan", *Carbohydrate Polymers, 84*, 2011, 1350-1356.

[27]. N. Kamila Banu and T. Santhi, "Development of tri-metal oxide nano composite adsorbent for the removal of reactive yellow-15 from aqus. Soln"., *Int. J. of sci. & nature, vol. 4(3)*, 2013, 381-389.